

Article

Antibacterial Activity of Superhydrophobic-SiO₂ Coatings to Inhibit the Growth of *Escherichia coli* and *Staphylococcus aureus*

Betania Sánchez-Santamaria, Delfino Cornejo-Monroy, Imelda Olivas-Armendáriz, José Saúl Arias-Cerón, Alfredo Villanueva-Montellano, Elsa Ordoñez-Casanova, José Omar Dávalos-Ramírez, Erwin Adán Martínez-Gómez and Jesús Manuel Jaquez-Muñoz

Special Issue

Synthesis and Applications of Bioactive Coatings

Edited by
Dr. Shenglian Yao



Article

Antibacterial Activity of Superhydrophobic-SiO₂ Coatings to Inhibit the Growth of *Escherichia coli* and *Staphylococcus aureus*

Betania Sánchez-Santamaria ¹, Delfino Cornejo-Monroy ^{1,*}, Imelda Olivas-Armendáriz ¹,
 José Saúl Arias-Cerón ², Alfredo Villanueva-Montellano ¹, Elsa Ordoñez-Casanova ¹,
 José Omar Dávalos-Ramírez ¹, Erwin Adán Martínez-Gómez ¹ and Jesús Manuel Jaquez-Muñoz ^{1,*}

- ¹ Instituto de Ingeniería y Tecnología, Universidad Autónoma de Ciudad Juárez, Ciudad Juárez 32310, Chihuahua, Mexico; betania.sanchez@uacj.mx (B.S.-S.); iolivas@uacj.mx (I.O.-A.); alfredo.villanueva@uacj.mx (A.V.-M.); eordonez@uacj.mx (E.O.-C.); jose.davalos@uacj.mx (J.O.D.-R.); emartine@uacj.mx (E.A.M.-G.)
- ² Engineering Department, Universidad Popular Autónoma del Estado de Puebla, Puebla 72410, Puebla, Mexico; josesaul.arias@upaep.mx
- * Correspondence: delfino.cornejo@uacj.mx (D.C.-M.); jesus.jaquezmn@uanl.edu.mx (J.M.J.-M.); Tel.: +52-656-556-3959 (J.M.J.-M.)

Abstract: The emergence of superhydrophobic antibacterial materials represents a promising approach to maintaining surface cleanliness and hygiene by effectively preventing bacterial adhesion. This research outlines the synthesis of a superhydrophobic coating with anti-adhesion and bacteriostatic properties, utilizing silica nanoparticles (SiO₂ NPs) modified with 1H,1H,2H,2H-Perfluorodecyltriethoxysilane (PFDTES). Transmission electron microscopy (TEM), X-ray diffraction (XRD), energy-dispersive X-ray spectroscopy (EDS), scanning electron microscopy (SEM), and Fourier-transform infrared (FTIR) spectroscopy were conducted to analyze the coating's morphology and surface characteristics. The coating was applied to glass substrates using the spray coating method, and the number of layers was varied to evaluate its antibacterial and bacteriostatic properties. These properties were measured using turbidimetry and inhibition halo techniques. Additionally, the durability of the coatings was assessed by exposing them to outdoor conditions for 35 days. This study aimed to evaluate the antibacterial and bacteriostatic capacities of the superhydrophobic coating, along with its resistance to outdoor weathering. The results indicate that a superhydrophobic coating with a contact angle $\geq 150^\circ$ and a sliding angle $\leq 10^\circ$ was successfully synthesized using SiO₂ NPs smaller than 10 nm, modified with PFDTES. The coating demonstrated an ability to inhibit bacterial growth by preventing the adhesion of bacteria such as *Escherichia coli* and *Staphylococcus aureus*. Furthermore, the number of coating layers significantly influenced its bacteriostatic efficacy. The coating also exhibited strong durability under outdoor conditions. These findings highlight the potential application of superhydrophobic coatings for the prevention of bacterial adhesion and growth in environments where such contamination poses risks.

Keywords: SiO₂ NPs; superhydrophobic coatings; SH-SiO₂ coating; PFDTES modification; antibacterial and bacteriostatic evaluation; biofilm prevention; nanotechnology; growth inhibition



Citation: Sánchez-Santamaria, B.; Cornejo-Monroy, D.; Olivas-Armendáriz, I.; Arias-Cerón, J.S.; Villanueva-Montellano, A.; Ordoñez-Casanova, E.; Dávalos-Ramírez, J.O.; Martínez-Gómez, E.A.; Jaquez-Muñoz, J.M. Antibacterial Activity of Superhydrophobic-SiO₂ Coatings to Inhibit the Growth of *Escherichia coli* and *Staphylococcus aureus*. *Coatings* **2024**, *14*, 1211. <https://doi.org/10.3390/coatings14091211>

Academic Editor: Shenglian Yao

Received: 14 August 2024

Revised: 12 September 2024

Accepted: 18 September 2024

Published: 20 September 2024



Copyright: © 2024 by the authors. Licensee MDPI, Basel, Switzerland. This article is an open access article distributed under the terms and conditions of the Creative Commons Attribution (CC BY) license (<https://creativecommons.org/licenses/by/4.0/>).

1. Introduction

The research and development of bacteria-repellent coatings has become a priority in enhancing safety within hospital environments [1]. Microbial fouling can lead to nosocomial infections when bacterial biofilms adhere to medical devices, a significant cause of transmission among patients [2–4]. *Escherichia coli* and *Staphylococcus* are among the most common pathogens involved in hospital-acquired infections [5], presenting significant challenges due to their resistance to antimicrobial treatments and their ability to persist on surfaces for extended periods, increasing the risk of transmission [6–8].

Preventing bacterial adhesion is crucial for the avoidance of infections and ensuring safety in clinical settings. Although biocides are commonly used to prevent or control bacterial growth, their frequent use raises concerns about the development of higher bacterial resistance and cross-resistance to clinically important antibiotics, leading to significant complications [9,10]. Biomimetic designs, which mimic natural structures like the micro- and nanoscale patterns found on lotus leaves, offer an innovative approach to creating superhydrophobic surfaces that can repel water and reduce microbial adherence [11]. For medical and industrial applications, the mechanism of action of self-cleaning surfaces is of great interest. Superhydrophobicity is explained by two physical principles: low surface energy and microscopic roughness. Surface chemistry and topography are the primary factors influencing liquid–solid interface interactions. Surface energy affects the adhesion of substances to the interface, including fluids and microorganisms.

Anti-adhesive and antibacterial coatings based on superhydrophobic functional surfaces can effectively prevent the non-specific adhesion of biomolecules, such as proteins, on material surfaces. Additionally, these coatings reduce initial bacterial adherence and inhibit the formation of bacterial biofilms, thereby achieving significant antibacterial effects [12]. However, further research is needed to fully understand the resistance mechanisms in biofilms, as bacteria in these environments can develop complex defenses, complicating their elimination [8].

In this context, developing antibacterial materials based on superhydrophobicity presents a promising strategy for maintaining clean and hygienic surfaces while preventing bacterial adhesion [1,2,5,13,14]. Although superhydrophilic surfaces may induce mechanical bacterial killing [15], superhydrophobic coatings using silica nanoparticles modified with PFDTES offer additional advantages, such as self-cleaning properties and resistance to biofilm formation. Understanding how *Escherichia coli* and *Staphylococcus aureus* interact with superhydrophobic surfaces is essential for developing effective strategies to prevent device-associated infections in healthcare settings [16–18].

Superhydrophobic surfaces, characterized by a water contact angle (WCA) greater than 150° and a water sliding angle (WSA) lower than 10° , repel water and enable a self-cleaning function by facilitating the removal of debris and pathogens [16,19]. Various methods can achieve these properties, including coatings designed with multiple layers of material to enhance functionality [20]. Consequently, these superhydrophobic coatings aim to prevent bacterial adhesion, inhibit bacterial growth, and allow for the easy removal of contaminants from surfaces [1].

Superhydrophobic coatings are based on compounds with low surface energy and high roughness [21,22]. A promising method for obtaining these coatings is the synthesis of modified SiO₂ nanoparticles (SiO₂ NPs) [23–25] which can be applied via the spray coating method [26]. SiO₂ NPs are potent nanocarriers with demonstrated antimicrobial properties and drug-delivery capabilities [27]. Due to their free silanol groups, which allow for modification, and their porous nature, which enables higher drug loading, SiO₂ NPs offer a viable alternative for infection treatment [12]. Additionally, the roughness of these nanoparticles can significantly influence their antibacterial properties, with greater roughness correlating with increased antibacterial effectiveness [28].

Moreover, the durability and stability of superhydrophobic coatings are critical under various environmental conditions, including outdoor exposure. Studies have shown that factors such as layer thickness, particle size, and the nature of functional groups play key roles in determining these properties [29]. Recent research also indicates that SiO₂ NPs modified with PFDTES exhibit high resistance to water abrasion and other environmental factors [30].

Our research focuses on developing a superhydrophobic coating with antibacterial properties for surfaces using SiO₂ NPs smaller than 10 nm, modified with PFDTES. The antibacterial activity was evaluated by applying the coating to glass substrates via the spray coating method, varying the number of layers, and using turbidimetry and inhibition halo techniques against *Escherichia coli* and *Staphylococcus aureus*. Additionally, coating

durability was analyzed via 35 days of outdoor exposure, and its morphology, composition, and hydrophobic properties were characterized. These findings confirm its effectiveness in preventing bacterial adhesion and growth, making it a promising strategy for areas where these bacteria pose a risk.

2. Methodology

2.1. Materials

To synthesize SiO₂ nanoparticles (NPs), tetraethyl orthosilicate (TEOS, Si(OC₂H₅)₄, 98%) was purchased from Sigma-Aldrich (Toluca, Mexico) and was utilized as the silica precursor. Ammonium hydroxide (NH₄OH, 28%–30% NH₃) by Sigma-Aldrich (Toluca, Mexico) was the catalyst agent. Isopropyl alcohol (C₃H₈O), from CEDROSA (Naucalpan de Juárez, Mexico) and deionized water (18 MΩ·cm) were employed as solvents for the hydrolysis process. For the modification of SiO₂ NPs and the preparation of the superhydrophobic coating, 1H,1H,2H,2H-Perfluorodecyltriethoxysilane (PFDTES, C₁₆H₁₉F₁₇O₃Si, 97%) was acquired from Matrix Scientific (Columbia, SC, USA) and was used along with hexane (C₆H₁₄, 95%) from J.T. Baker (Xalostoc, Mexico) as the solvent. Glass substrates used for the deposition and analysis of the coating were obtained from LAUKA (Iztalapa, Mexico).

2.2. Equipment

The synthesis and characterization of the superhydrophobic coatings were carried out using the following equipment: a laboratory stirrer PC 410, Corning (Lowell, MA, USA) for solution mixing and a water purification system Water-Pro PS (Labconco (Kansas, MI, USA)) for the production of deionized water. Fourier-transform infrared (FTIR) spectroscopy analysis was conducted using an infrared spectrometer NICOLET IS50 FT-IR Thermo Scientific (Waltham, MA, USA). X-ray diffraction (XRD) analysis was performed with a diffractometer X'Pert Pro Panalytical (Almelo, The Netherlands). Transmission electron microscopy (TEM) characterization was carried out using a transmission electron microscope JEM-2010, JEOL (Akishima, Japan), with samples deposited on carbon-coated copper grids from Ted Pella Inc. Finally, scanning electron microscopy (SEM) was performed using a scanning electron microscope JSM-7401, JEOL (Akishima, Japan).

2.3. Synthesis and Characterization

The synthesis of silica nanoparticles (SiO₂ NPs) followed the method proposed by Stöber [31]. To prepare a 100 mL solution of SiO₂ NPs, 95 mL of isopropyl alcohol was stirred at 300 rpm. Subsequently, 3.65 mL of deionized water, 350 µL of NH₄OH, and 1 mL of TEOS were added. The mixture was maintained at 40 °C under continuous stirring for 24 h. After this period, 25 mL of hexane was introduced into the solution, the temperature was increased to 60 °C, and 500 µL of PFDTES was added. The solution was stirred at 300 rpm for an additional 48 h, producing 125 mL of superhydrophobic coating.

For the coating application, 1, 3, 5, and 7 layers of the superhydrophobic coating were deposited onto glass substrates using the spray coating technique. This process was carried out at an air pressure of 30 psi, with a 15 cm distance between the nozzle and the substrate. The samples were then exposed to outdoor conditions for 35 days to evaluate changes in surface superhydrophobicity. The water contact angle (WCA) and the water sliding angle (WSA) of the coating were characterized using custom-built laboratory equipment at room temperature. Deionized water droplets of 4 µL were used for the measurements, and the contact angle was measured five times at different positions on each sample to obtain an average value.

For FTIR and XRD characterization, the solutions were evaporated to obtain the SiO₂ NPs and the superhydrophobic coating in powder form. These powders were deposited onto glass slides for subsequent analysis. For SEM and EDS analysis, glass substrates with varying numbers of coating layers were examined. For TEM analysis, the colloidal samples were deposited onto carbon-coated copper grids.

2.4. Antibacterial and Bacteriostatic Study

The antibacterial and bacteriostatic study of the superhydrophobic coating involved depositing 1, 3, 5, and 7 layers onto glass substrates using the spray coating method.

For the antibacterial test, the turbidimetry technique was employed using 1:1 solutions (culture broth–phosphate-buffered solution) containing *Escherichia coli* (ATCC[®] 11229[™]) and *Staphylococcus aureus* (ATCC[®] 6538[™]). The tests were conducted by adding the bacterial solution to tubes containing the coated samples, followed by incubation at 37 °C for 24 h in a Fisher Scientific Low-Temperature Incubator. After incubation, the solutions were measured at a wavelength of 450 nm using UV–visible spectroscopy (Genesys2, Thermo Spectronic). Negative controls (bacterial solution without a sample) and positive controls (buffer solution with a sample) were included, and the analysis was performed in triplicate.

Prior to testing, all samples were sterilized using UV light within a laminar flow hood (Labconco) for 15 min on each side. Additionally, the inhibition halo zone method was employed to analyze the antibacterial properties according to ASTM E2149. A nutrient agar medium (Difco 21300) was prepared, sterilized, and poured into Petri dishes to solidify. Bacterial suspensions of *Escherichia coli* (ATCC[®] 11229[™]) and *Staphylococcus aureus* (ATCC[®] 6538[™]) at densities of 1.5×10^8 CFU/mL were prepared and evenly spread over the agar surface in the Petri dishes using the streaking technique. The samples were then placed onto the inoculated agar, and the Petri dishes were incubated at 37 °C for 24 and 48 h to observe the formation of inhibition halos.

3. Results

3.1. WCA and WSA

The manufactured coating exhibited water contact angles (WCA) of $\geq 150^\circ$ and water sliding angles (WSA) of $\leq 10^\circ$. Figure 1 shows photographs of water droplets deposited on glass substrates with varying numbers of coating layers. Table 1 provides the initial contact and sliding angle values, as well as those measured after 35 days of exposure to outdoor conditions.

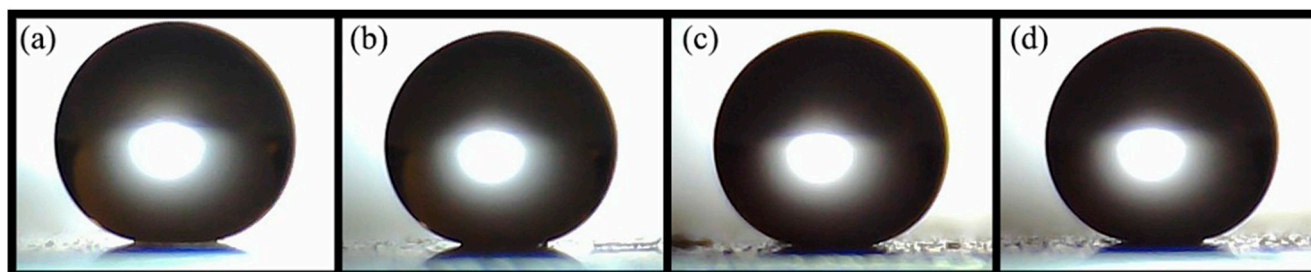


Figure 1. Images of water droplets on glass substrates with varying numbers of superhydrophobic coating layers: (a) 1 layer, (b) 3 layers, (c) 5 layers, and (d) 7 layers.

Initially, as the number of layers increases, the WCA also increases, while the WSA remains below 3° , demonstrating the necessary characteristics for superhydrophobicity. The increase in WCA with additional coating layers is primarily attributed to the enhanced surface roughness and hierarchical structure imparted by these layers. According to the Cassie–Baxter model, surfaces with greater roughness and air pockets trap more air beneath the water droplet, thereby increasing the apparent contact angle. The multilayered structure improves the surface’s ability to repel water, resulting in higher WCA values [32].

After 35 days, the coating retains contact angles $\geq 150^\circ$ and sliding angles $\leq 10^\circ$. This stability may be explained by potential surface reorganization or further chemical reactions under environmental conditions. Outdoor exposure often leads to the rearrangement of low-surface-energy compounds, such as the perfluorodecyltriethoxysilane (PFDTES) used in the coating. This rearrangement can further lower the surface energy, contributing to the observed increase in WCA. Additionally, environmental factors such as UV radiation

and temperature fluctuations may induce minor surface oxidation, which can enhance hydrophobicity through the formation of stable surface chemistry [33].

Table 1. WCA and WSA values of superhydrophobic coatings with varying layers were measured initially and after 35 days of outdoor exposure.

Layers	WCA	WSA
1	$156.72^\circ \pm 1.01^\circ$	$2.64^\circ \pm 0.55^\circ$
3	$157.01^\circ \pm 1.76^\circ$	$2.01^\circ \pm 0.15^\circ$
5	$157.49^\circ \pm 1.07^\circ$	$2.21^\circ \pm 0.17^\circ$
7	$159.92^\circ \pm 1.03^\circ$	$2.13^\circ \pm 0.61^\circ$
After 35 days of outdoor exposure		
Layers	WCA	WSA
1	$159.78^\circ \pm 1.07^\circ$	$2.91^\circ \pm 0.10^\circ$
3	$160.50^\circ \pm 1.17^\circ$	$2.27^\circ \pm 0.29^\circ$
5	$157.60^\circ \pm 1.05^\circ$	$2.17^\circ \pm 0.94^\circ$
7	$160.75^\circ \pm 1.01^\circ$	$2.94^\circ \pm 0.71^\circ$

3.2. SEM

Figures 2 and 3 show the morphology of the coatings on glass substrates with varying numbers of layers. Scanning electron microscopy observations in both figures reveal surfaces with a hierarchical structure composed of nano- and microscale particles with diameters ranging from 733.5 ± 116.9 nm to 20.046 ± 3.69 nm. This multiscale roughness is advantageous for superhydrophobic coatings, enhancing superhydrophobicity, durability, and self-cleaning properties [21].

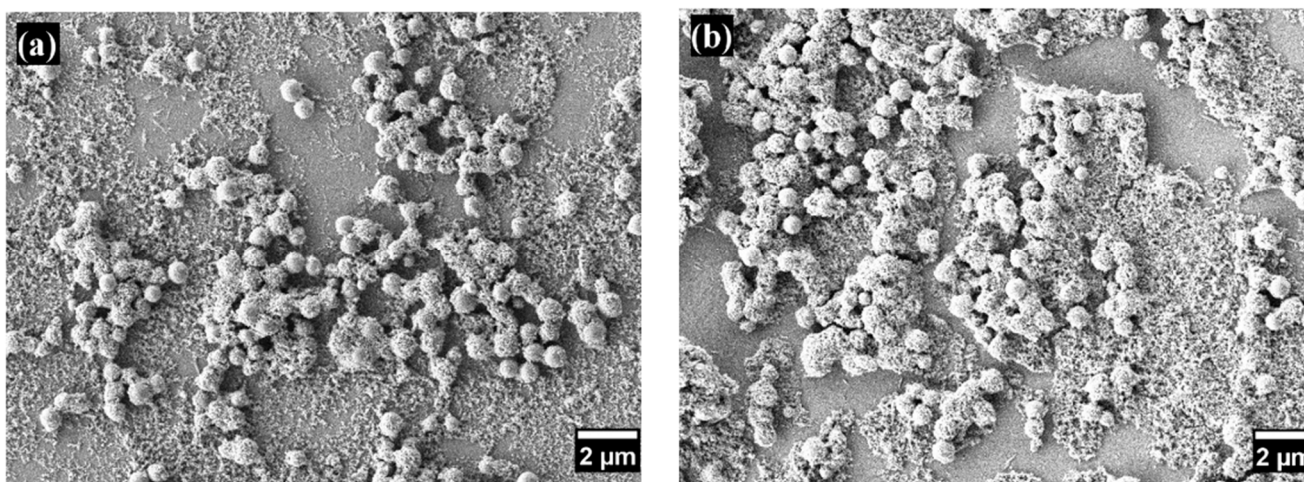


Figure 2. SEM images of superhydrophobic coatings with different numbers of layers: (a) one layer and (b) seven layers.

Figure 3 provides a detailed view of the increased porosity corresponding to the additional coating layers. This enhanced porosity allows for more effective air trapping beneath water droplets, significantly contributing to the surface's superhydrophobic properties.

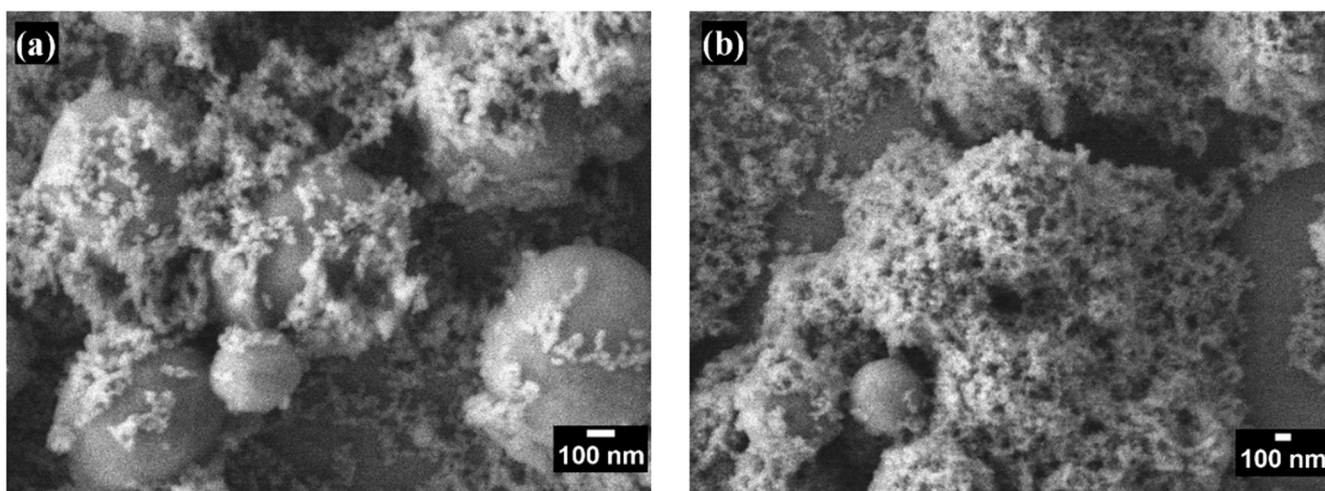


Figure 3. High-magnification SEM images of superhydrophobic coatings with different numbers of layers: (a) one layer and (b) seven layers.

3.3. TEM

TEM images of the colloids are presented in Figure 4. Figure 4a shows bare SiO₂ NPs, which are spherical, well-dispersed, and relatively uniform, with an average size of 6.309 ± 1.891 nm. In contrast, Figure 4b,c display the superhydrophobic coating at different magnifications. These images reveal a hierarchical structure of the material, confirming the presence of particles at both the micro- and nanoscale with diameters ranging from 658 ± 89.5 nm to 17.49 ± 4.83 nm.

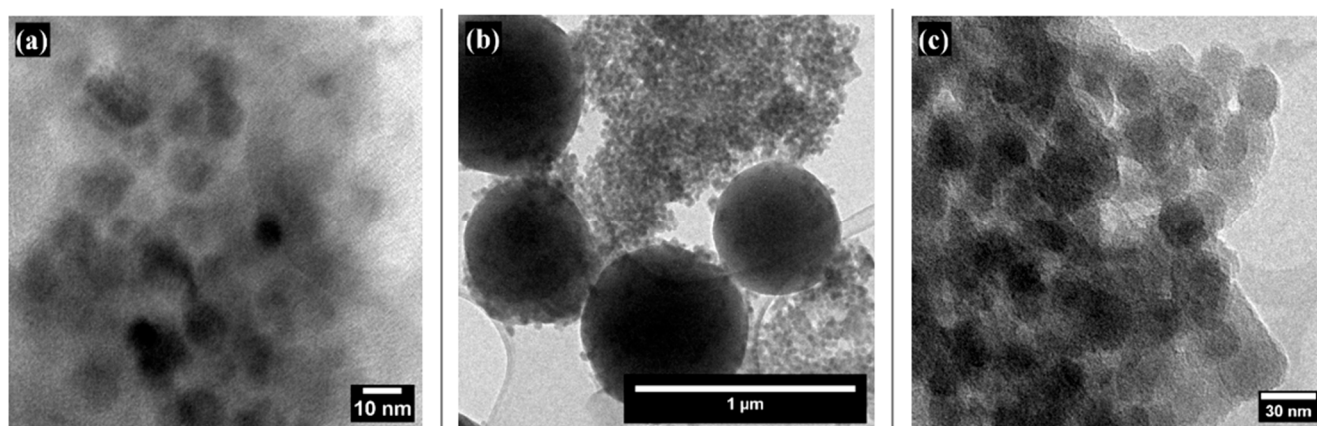


Figure 4. TEM images of SiO₂ and SiO₂ NPs modified with PFDTES at different magnifications: (a) bare SiO₂ NPs, (b) SiO₂ NPs modified with PFDTES showing both micro- and nanoparticles, and (c) SiO₂ NPs modified with PFDTES at high magnification.

3.4. EDS

The energy-dispersive X-ray spectroscopy (EDS) analysis in Figure 5 confirmed the presence of fluorine and carbon, indicating the successful modification of the nanoparticles with trifluoromethyl (CF₃) groups. These findings verify the incorporation of the desired functional groups onto the surface of the silica nanoparticles, thereby confirming the functionalization and effectiveness of the superhydrophobic coating.

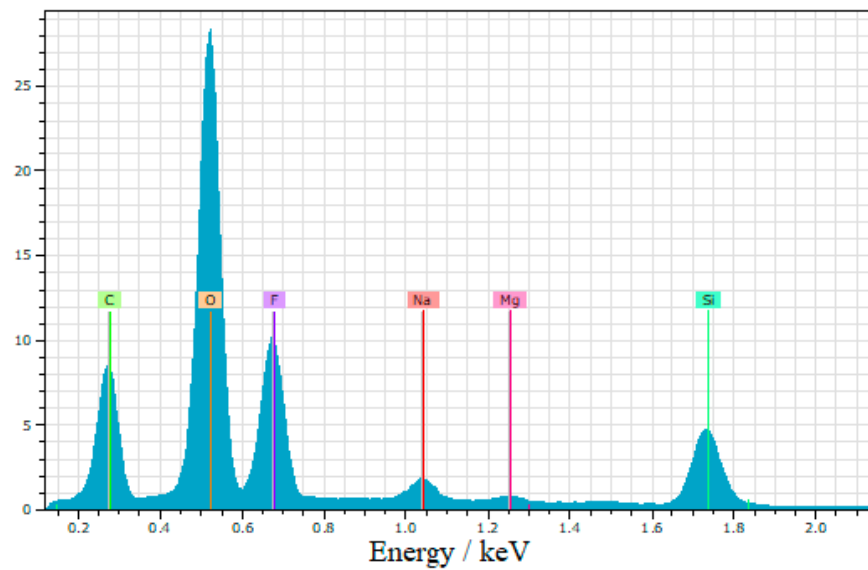


Figure 5. EDS spectra of superhydrophobic coating.

3.5. FTIR Spectroscopy

Figure 6 shows the infrared spectra of SiO_2 NPs and the superhydrophobic coating. The infrared spectrum of the SiO_2 NPs exhibits peaks at 1055 cm^{-1} , 955 cm^{-1} , and 796 cm^{-1} , corresponding to the fingerprint region of silica [34]. Both spectra also display signals at 442 cm^{-1} and 560 cm^{-1} attributed to the bending vibrations of O-Si-O, which are typical in amorphous silica [35].

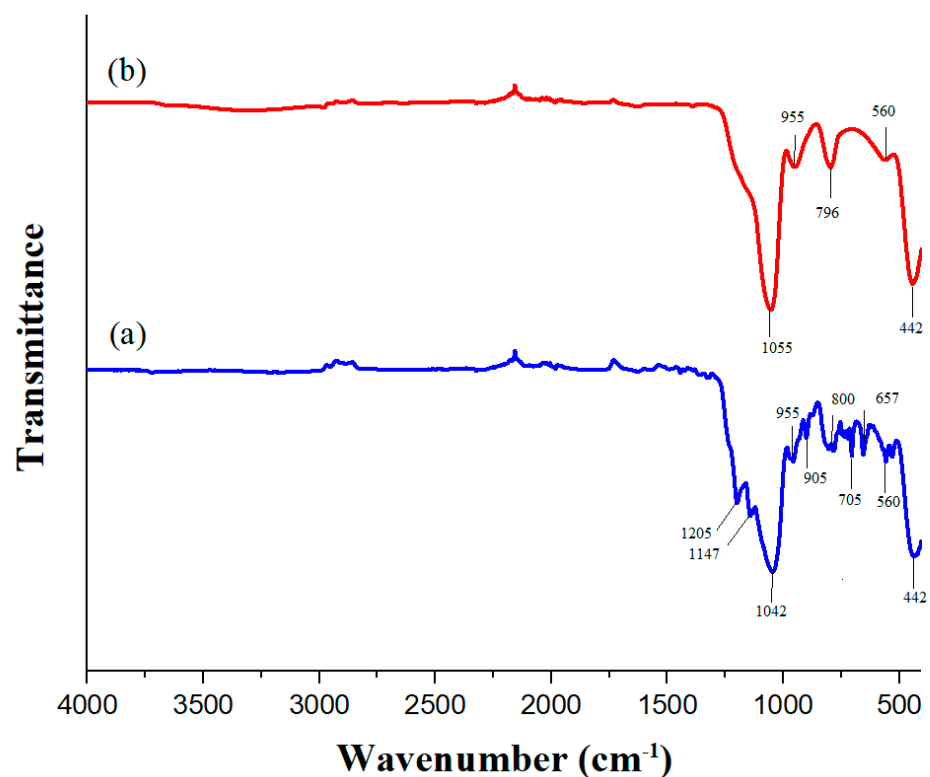


Figure 6. FT-IR spectra of (a) SiO_2 NPs and (b) superhydrophobic coating.

The FTIR spectrum of the coating reveals additional peaks, such as those at 1205 cm^{-1} and 1147 cm^{-1} , which are likely indicative of C-F stretching vibrations [36,37]. The peak at 1042 cm^{-1} confirms the presence of SiO_2 , while the peaks at 905 cm^{-1} , 800 cm^{-1} , 705 cm^{-1} ,

and 657 cm^{-1} are assigned to the symmetric stretching vibrations of Si-O-Si due to functionalization [38]. These functional groups are essential for ensuring the superhydrophobicity of the nanoparticles and confirming successful nanoparticle functionalization.

3.6. XRD

As shown in Figure 7, the X-ray diffraction (XRD) pattern of the SiO₂ NPs exhibits an amorphous structure consistent with the JCPDS file 00-083-2467. The broad peak observed at a Bragg angle of $2\theta = 23.37^\circ$ is characteristic of amorphous materials, including amorphous silica [39].

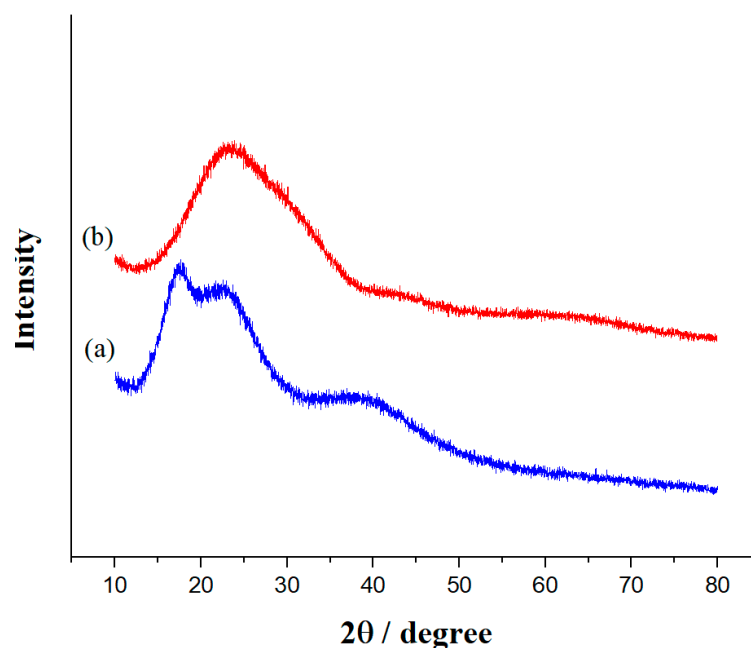


Figure 7. XRD patterns of (a) SiO₂ NPs and (b) the superhydrophobic coating.

Post functionalization, the XRD pattern reveals the persistence of the amorphous nature of SiO₂, along with the emergence of three new peaks at $2\theta = 17.67^\circ$, 22.72° , and 39.44° . These new peaks suggest the formation of a crystalline phase or a structural change due to the functionalization process. Such changes may result from compressive or expansive stresses within the material, affecting the diffraction angles. Additionally, the introduction of C-F groups on the surface of SiO₂ can alter the local atomic environment, leading to variations in peak intensities, the appearance of new peaks, or shifts in existing peaks [36].

Furthermore, the hydrophobic nature of the C-F groups can reduce interactions with surrounding water molecules, potentially causing changes in the nanoparticle structure. This may lead to aggregation or changes in particle morphology [40].

3.7. Antimicrobial Activity

Figure 8 presents the antibacterial activity of various samples measured using the turbidimetry technique. The data show that the percentage of antibacterial activity against *Escherichia coli* and *Staphylococcus aureus* increased with the number of coating layers, reaching 11.37% and 12.58%, respectively. *Escherichia coli*, a Gram-negative bacterium, has two membranes, while *Staphylococcus aureus*, a Gram-positive bacterium, has a thick cell wall, contributing to its resistance mechanisms against antibacterial substances. Nevertheless, the coating exhibited antibacterial activity against both types of bacteria, with the highest activity observed against the Gram-positive bacteria.

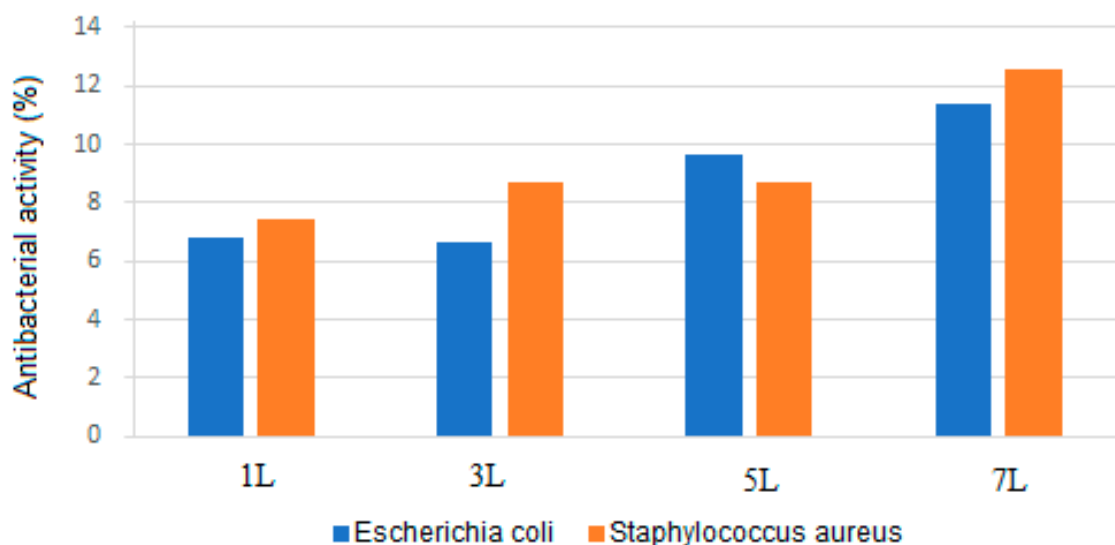
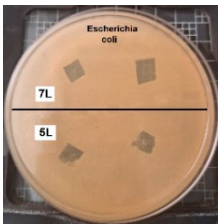
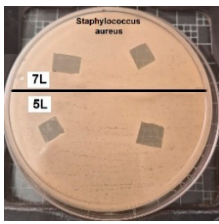
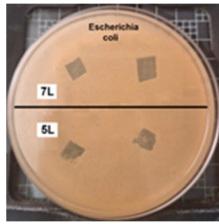
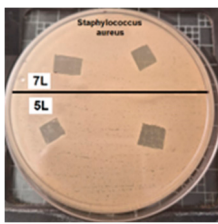
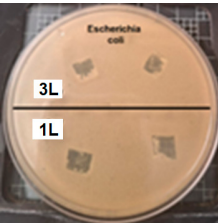
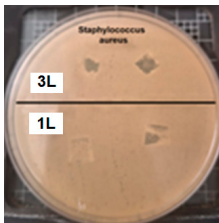
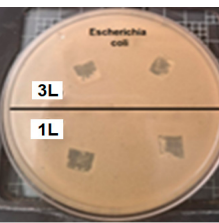
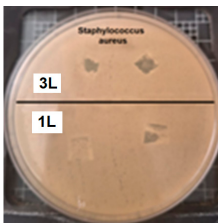


Figure 8. Graphical representation of the antibacterial activity of samples with different numbers of superhydrophobic coating layers: 1 L (one layer), 3 L (three layers), 5 L (five layers), and 7 L (seven layers) after 24 h of exposure to *Escherichia coli* and *Staphylococcus aureus*.

Table 2 presents the results of antibacterial activity measured by the inhibition halo. No inhibition halos were formed in any of the samples, indicating that the surfaces do not necessarily kill bacteria. However, what is evident (Figure 9) on the superhydrophobic coating, particularly those with seven layers (7 L) and five layers (5 L), is the inhibition of bacterial growth and reproduction. This behavior is indicative of bacteriostatic properties, consistent with the findings of Zhou et al. [41,42].

Table 2. Antibacterial activity of samples with varying numbers of layers (1 L to 7 L) after 24 and 48 h of exposure to *Escherichia coli* and *Staphylococcus aureus*.

	<i>Escherichia coli</i> 24 h	<i>Staphylococcus aureus</i> 24 h	<i>Escherichia coli</i> 48 h	<i>Staphylococcus aureus</i> 48 h
7 L and 5 L				
3 L and 1 L				

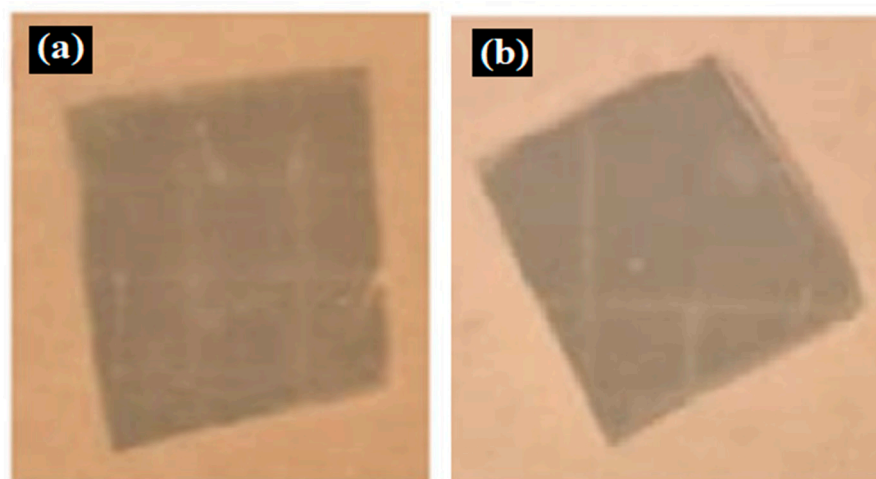


Figure 9. Enlarged images from Table 2 showing inhibition halo test results for samples with (a) *Escherichia coli* (7 layers) and (b) *Staphylococcus aureus* (7 layers) bacteria after 48 h.

4. Discussion

The water contact angle (WCA) results ranged from 156° to 159° when the coating was not exposed to outdoor conditions, with values increasing as the number of layers increased. Other studies have reported WCA results between 125° and 160° for silicone-based coatings, which aligns with the values obtained in this study. The increase in WCA after 35 days of exposure may be attributed to chemical polymerization of the hydrophobic membrane [19,24,25,27,31,38].

The hierarchical structure of our coating helps maintain water droplets in place [43]. Developing hydrophobic coatings critically depends on the creation of hierarchical structures and surface roughness. The 35-day exposure likely altered the coating roughness, resulting in a more hydrophobic layer [44].

Previous studies have used PFDTES in combination with a nano-hierarchical structure to inhibit bacterial adhesion [44]. The hierarchical structure appears to reduce bacterial proliferation, influenced by the structure's size, as reflected in the TEM results: 6.309 ± 1.891 nm and 658 ± 89.5 nm to 17.49 ± 4.83 nm [8,10,14,24,27,38,39,45–47].

The hierarchical structure of our coating, which includes nano- and microscale features, significantly increases surface roughness, contributing to its superhydrophobicity, characterized by water contact angles above 150° and sliding angles below 10° . This high surface roughness, combined with the low surface energy imparted by PFDTES modification, creates an unfavorable environment for bacterial adhesion, thereby preventing biofilm formation [14]. Moreover, the coating serves as a physical barrier, repelling water droplets that may carry bacteria and inhibiting their ability to colonize. The modified SiO_2 nanoparticles in the coating may further interfere with bacterial cellular functions, such as DNA replication, leading to bacteriostasis. Additionally, the incorporation of trifluoromethyl (CF_3) groups introduces a hydrophobic, chemically inert surface that reduces surface energy, making the coating hostile to bacteria like *Staphylococcus aureus*, thereby enhancing its antimicrobial properties [43,48,49]. The results indicate that the concentration of coating layers significantly influences bacteriostatic efficacy.

The antibacterial properties of superhydrophobic coatings have been extensively studied, particularly in relation to preventing bacterial adhesion and biofilm formation. Our study builds upon this foundation by utilizing silica nanoparticles (SiO_2 NPs) modified with 1H,1H,2H,2H-Perfluorodecyltriethoxysilane (PFDTES) to create a superhydrophobic coating. In contrast to the bactericidal mechanisms described by Dimitrakellis et al. [15], who used smooth and plasma micro-/nanotextured surfaces incorporating copper (Cu) as a biocidal agent, our approach primarily relies on surface roughness and chemical modification to achieve bacteriostatic effects, without the need for active biocides. This

distinction is significant because, while Cu-based surfaces actively kill bacteria, our coating inhibits bacterial growth by preventing adhesion.

Additionally, the work by Jin et al. [50] on nanodarts and nanoblades demonstrates a mechano-bactericidal approach, where sharp nanostructures physically rupture bacterial cells. In contrast, our superhydrophobic coating does not directly kill bacteria but inhibits their proliferation by repelling water and creating an unfavorable surface for colonization. This non-invasive, durable antibacterial strategy is well-suited for applications where mechanical damage to bacteria is undesirable.

Our findings also emphasize the importance of durability under environmental conditions, a feature that has not been extensively tested in the aforementioned studies. The 35-day outdoor exposure test demonstrated that our coating's superhydrophobic properties were retained, underscoring its potential for long-term use in outdoor or industrial settings. While Dimitrakellis et al. focus on chemical resistance through plasma treatment, our study shows that surface roughness, when combined with chemical modification, is sufficient to maintain functionality under environmental stress.

5. Conclusions

The developed superhydrophobic coating demonstrates significant antibacterial activity, particularly against Gram-positive bacteria. Additionally, all samples exhibited bacteriostatic activity, indicating the coating's effectiveness in inhibiting bacterial growth on the treated surface. The antibacterial activity of the coating was influenced by the number of layers, with samples containing more layers displaying greater effectiveness.

Morphological and structural characterization revealed a hierarchical structure in the coating, with nano- and microscale particles contributing to its roughness and superhydrophobicity, evidenced by contact angles $\geq 150^\circ$ and sliding angles $\leq 10^\circ$. The increase in WCA with the addition of more layers is due to enhanced surface roughness and hierarchical structuring, while the changes after outdoor exposure are likely the result of surface reorganization and possible chemical reactions that further stabilize the hydrophobic surface.

The successful functionalization of silica nanoparticles with trifluoromethyl (CF₃) groups in the coating confirms the efficacy of the functionalization and the coating's ability to repel water and resist biofilm formation.

These findings suggest that the superhydrophobic coating holds significant promise for applications requiring clean surfaces, resistance to biofilm formation, and effective antibacterial properties.

Author Contributions: Conceptualization, B.S.-S., D.C.-M. and I.O.-A.; methodology, D.C.-M. and A.V.-M.; validation, J.S.A.-C., I.O.-A. and D.C.-M.; formal analysis, D.C.-M.; investigation, E.A.M.-G., J.S.A.-C., E.O.-C. and J.O.D.-R.; resources, E.A.M.-G.; data curation, B.S.-S. and D.C.-M.; writing—original draft preparation, B.S.-S.; writing—review and editing, J.M.J.-M. and D.C.-M.; visualization, B.S.-S.; supervision, I.O.-A.; project administration, D.C.-M. All authors have read and agreed to the published version of the manuscript.

Funding: This research received no external funding.

Institutional Review Board Statement: Not applicable.

Informed Consent Statement: Not applicable.

Data Availability Statement: Data are contained within the article.

Conflicts of Interest: The authors declare no conflicts of interest.

References

1. Privett, B.J.; Youn, J.; Hong, S.A.; Lee, J.; Han, J.; Shin, J.H.; Schoenfisch, M.H. Antibacterial fluorinated silica colloid superhydrophobic surfaces. *Langmuir* **2011**, *27*, 9597–9601. [[CrossRef](#)] [[PubMed](#)]
2. Ashok, D.; Taheri, M.; Garg, P.; Webb, D.; Parajuli, P.; Wang, Y.; Funnell, B.; Taylor, B.; Tschärke, D.C.; Tsuzuki, T.; et al. Shielding surfaces from viruses and bacteria with a multiscale coating. *Adv. Sci.* **2022**, *9*, 2201415. [[CrossRef](#)] [[PubMed](#)]

3. Schmidt, M.G.; Attaway, H.H.; Sharpe, P.A.; John, J.; Sepkowitz, K.A.; Morgan, A.; Fairey, S.E.; Singh, S.; Steed, L.L.; Cantey, J.R.; et al. Sustained reduction of microbial burden on common hospital surfaces through introduction of copper. *J. Clin. Microbiol.* **2012**, *50*, 2217–2223. [[CrossRef](#)] [[PubMed](#)]
4. Zarb, P.; Coignard, B.; Griskeviciene, J.; Muller, A.; Vankerckhoven, V.; Weist, K.; Goossens, M.; Vaerenberg, S.; Hopkins, S.; Catry, B.; et al. The European Centre for Disease Prevention and Control (ECDC) pilot point prevalence survey of healthcare-associated infections and antimicrobial use. *Eurosurveillance* **2012**, *17*, 20316. [[CrossRef](#)]
5. Ashok, D.; Cheeseman, S.; Wang, Y.; Funnell, B.; Leung, S.-F.; Tricoli, A.; Nisbet, D. Superhydrophobic surfaces to combat bacterial surface colonization. *Adv. Mater. Interfaces* **2023**, *10*, 2300324. [[CrossRef](#)]
6. Donlan, R.M. Biofilms: Microbial life on surfaces. *Emerg. Infect. Dis.* **2002**, *8*, 881–890. [[CrossRef](#)]
7. Kokare, C.R.; Chakraborty, S.; Khopade, A.N.; Mahadik, K.R. Biofilm: Importance and applications. *Indian J. Biotechnol.* **2009**, *8*, 159–168.
8. Stewart, P.S.; Costerton, J.W. Antibiotic resistance of bacteria in biofilms. *Lancet* **2001**, *358*, 135–138. [[CrossRef](#)]
9. Poole, K. Mechanisms of bacterial biocide and antibiotic resistance. *J. Appl. Microbiol.* **2002**, *92* (Suppl. S1), 55s–64s. [[CrossRef](#)]
10. Zhang, X.; Wang, L.; Levänen, E. Superhydrophobic surfaces for the reduction of bacterial adhesion. *RSC Adv.* **2013**, *3*, 12003–12020. [[CrossRef](#)]
11. Zhang, C.; McAdams, D.A., 2nd; Grunlan, J.C. Nano/micro-manufacturing of bioinspired materials: A review of methods to mimic natural structures. *Adv. Mater.* **2016**, *28*, 6292–6321. [[CrossRef](#)] [[PubMed](#)]
12. Wang, L.; Guo, X.; Zhang, H.; Liu, Y.; Wang, Y.; Liu, K.; Liang, H.; Ming, W. Recent advances in superhydrophobic and antibacterial coatings for biomedical materials. *Coatings* **2022**, *12*, 1469. [[CrossRef](#)]
13. Berendjchi, A.; Khajavi, R.; Yazdanshenas, M.E. Fabrication of superhydrophobic and antibacterial surface on cotton fabric by doped silica-based sols with nanoparticles of copper. *Nanoscale Res. Lett.* **2011**, *6*, 594. [[CrossRef](#)] [[PubMed](#)]
14. Falde, E.J.; Yohe, S.T.; Colson, Y.L.; Grinstaff, M.W. Superhydrophobic materials for biomedical applications. *Biomaterials* **2016**, *104*, 87–103. [[CrossRef](#)]
15. Dimitrakellis, P.; Ellinas, K.; Kaprou, G.D.; Mastellos, D.C.; Tserepi, A.; Gogolides, E. Bactericidal action of smooth and plasma micro-nanotextured polymeric surfaces with varying wettability, enhanced by incorporation of a biocidal agent. *Macromol. Mater. Eng.* **2021**, *306*, 2000694. [[CrossRef](#)]
16. Ciasca, G.; Papi, M.; Businaro, L.; Campi, G.; Ortolani, M.; Palmieri, V.; Cedola, A.; De Ninno, A.; Gerardino, A.; Maulucci, G.; et al. Recent advances in superhydrophobic surfaces and their relevance to biology and medicine. *Bioinspir. Biomim.* **2016**, *11*, 011001. [[CrossRef](#)]
17. Crick, C.R.; Ismail, S.; Pratten, J.; Parkin, I.P. An investigation into bacterial attachment to an elastomeric superhydrophobic surface prepared via aerosol assisted deposition. *Thin Solid Film* **2011**, *519*, 3722–3727. [[CrossRef](#)]
18. Marmur, A. Super-hydrophobicity fundamentals: Implications to biofouling prevention. *Biofouling* **2006**, *22*, 107–115. [[CrossRef](#)]
19. Erbil, H.Y. Practical applications of superhydrophobic materials and coatings: Problems and perspectives. *Langmuir* **2020**, *36*, 2493–2509. [[CrossRef](#)]
20. Sreekantan, S.; Hassan, M.; Sundera Murthe, S.; Seeni, A. Biocompatibility and cytotoxicity study of polydimethylsiloxane (PDMS) and palm oil fuel ash (POFA) sustainable super-hydrophobic coating for biomedical applications. *Polymers* **2020**, *12*, 3034. [[CrossRef](#)]
21. Feng, L.; Li, S.; Li, Y.; Li, H.; Zhang, L.; Zhai, J.; Song, Y.; Liu, B.; Jiang, L.; Zhu, D. Super-hydrophobic surfaces: From natural to artificial. *Adv. Mater.* **2002**, *14*, 1857–1860. [[CrossRef](#)]
22. Mahadik, S.A.; Pedraza, F.; Mahadik, S.S.; Relekar, B.P.; Thorat, S.S. Biocompatible superhydrophobic coating material for biomedical applications. *J. Sol-Gel Sci. Technol.* **2017**, *81*, 791–796. [[CrossRef](#)]
23. Liang, Z.; Geng, M.; Dong, B.; Zhao, L.; Wang, S. Transparent and robust SiO₂/PDMS composite coatings with self-cleaning. *Surf. Eng.* **2020**, *36*, 643–650. [[CrossRef](#)]
24. Zhang, Z.; Xu, C.; Liu, W.; Wang, K.; Rao, Y.; Jiang, C.; Li, D.; Zhang, Y.; Jiang, X.; Chen, X.; et al. Ultrasonic assisted rapid preparation of superhydrophobic stainless steel surface and its application in oil/water separation. *Ultrason. Sonochem.* **2021**, *81*, 105848. [[CrossRef](#)]
25. Zhao, Y.; Huo, M.; Huo, J.; Zhang, P.; Shao, X.; Zhang, X. Preparation of silica-epoxy superhydrophobic coating with mechanical stability and multifunctional performance via one-step approach. *Colloids Surf. A Physicochem. Eng. Asp.* **2022**, *653*, 129957. [[CrossRef](#)]
26. Ye, H.; Zhu, L.; Li, W.; Liu, H.; Chen, H. Constructing fluorine-free and cost-effective superhydrophobic surface with normal-alcohol-modified hydrophobic SiO₂ nanoparticles. *ACS Appl. Mater. Interfaces* **2017**, *9*, 858–867. [[CrossRef](#)]
27. Alavi, M.; Thomas, S.; Sreedharan, M. Modification of silica nanoparticles for antibacterial activities: Mechanism of action. *Micronano Bio Asp.* **2022**, *1*, 49–58. [[CrossRef](#)]
28. Wang, F.; Pi, J.; Song, F.; Feng, R.; Xu, C.; Wang, X.-L.; Wang, Y.-Z. A superhydrophobic coating to create multi-functional materials with mechanical/chemical/physical robustness. *Chem. Eng. J.* **2020**, *381*, 122539. [[CrossRef](#)]
29. Xue, F.; Shi, X.; Bai, W.; Li, J.e.; Li, Y.; Zhu, S.; Liu, Y.; Feng, L. Enhanced durability and versatile superhydrophobic coatings via facile one-step spraying technique. *Colloids Surf. A Physicochem. Eng. Asp.* **2022**, *640*, 128411. [[CrossRef](#)]
30. Liu, X.; Zhou, Z.; Chen, M.; Liu, Z.; Jiang, S.; Wang, L. Preparation of durable superhydrophobic coatings based on discrete adhesives. *Coatings* **2024**, *14*, 463. [[CrossRef](#)]

31. Stöber, W.; Fink, A.; Bohn, E. Controlled growth of monodisperse silica spheres in the micron size range. *J. Colloid Interface Sci.* **1968**, *26*, 62–69. [[CrossRef](#)]
32. Quéré, D. Wetting and roughness. *Annu. Rev. Mater. Res.* **2008**, *38*, 71–99. [[CrossRef](#)]
33. Prakash, C.G.J.; Prasanth, R. Approaches to design a surface with tunable wettability: A review on surface properties. *J. Mater. Sci.* **2021**, *56*, 108–135. [[CrossRef](#)]
34. Stuart, B.H. *Infrared Spectroscopy: Fundamentals and Applications*; Wiley: Hoboken, NJ, USA, 2004.
35. Zhuravlev, L.T. The surface chemistry of amorphous silica. Zhuravlev model. *Colloids Surf. A Physicochem. Eng. Asp.* **2000**, *173*, 1–38. [[CrossRef](#)]
36. Lee, H.; Dellatore, S.M.; Miller, W.M.; Messersmith, P.B. Mussel-inspired surface chemistry for multifunctional coatings. *Science* **2007**, *318*, 426–430. [[CrossRef](#)] [[PubMed](#)]
37. Zhu, Y.; Murali, S.; Cai, W.; Li, X.; Suk, J.W.; Potts, J.R.; Ruoff, R.S. Graphene and graphene oxide: Synthesis, properties, and applications. *Adv. Mater.* **2010**, *22*, 3906–3924. [[CrossRef](#)]
38. Coates, J. Interpretation of Infrared Spectra, a Practical Approach. In *Encyclopedia of Analytical Chemistry*; Wiley: Chichester, UK, 2006.
39. Musić, S.; Filipović-Vinceković, N.; Sekovanić, L. Precipitation of amorphous SiO₂ particles and their properties. *Braz. J. Chem. Eng.* **2011**, *28*, 89–94. [[CrossRef](#)]
40. Cullity, B.D.; Stock, S.R. *Elements of X-ray Diffraction*, 3rd ed.; Pearson: Upper Saddle River, NJ, USA, 2014.
41. Das, P.; Ganguly, S.; Bose, M.; Mondal, S.; Choudhary, S.; Gangopadhyay, S.; Das, A.K.; Banerjee, S.; Das, N.C. Zinc and nitrogen ornamented bluish white luminescent carbon dots for engrossing bacteriostatic activity and Fenton based bio-sensor. *Mater. Sci. Eng. C* **2018**, *88*, 115–129. [[CrossRef](#)]
42. Zhou, H.; Persson, C.; Donzel-Gargand, O.; Engqvist, H.; Xia, W. Structural Si₃N₄-SiO₂ glass ceramics with bioactive and anti-bacterial properties. *J. Eur. Ceram. Soc.* **2024**, *44*, 4260–4271. [[CrossRef](#)]
43. Villegas, M.; Bayat, F.; Kramer, T.; Schwarz, E.; Wilson, D.; Hosseinidoust, Z.; Didar, T.F. Emerging strategies to prevent bacterial infections on titanium-based implants. *Small* **2024**, 2404351. [[CrossRef](#)]
44. Yu, M.; Cui, Z.; Ge, F.; Man, C.; Lei, L.; Wang, X. Fabrication of durable and roughness-regeneration superhydrophobic composite materials by hot pressing. *Compos. Part B Eng.* **2019**, *179*, 107431. [[CrossRef](#)]
45. Jia, W.; Kharraz, J.A.; Choi, P.J.; Guo, J.; Deka, B.J.; An, A.K. Superhydrophobic membrane by hierarchically structured PDMS-POSS electro spray coating with cauliflower-shaped beads for enhanced MD performance. *J. Membr. Sci.* **2020**, *597*, 117638. [[CrossRef](#)]
46. Sarkar, D.K.; Farzaneh, M.; Paynter, R.W. Superhydrophobic properties of ultrathin rf-sputtered Teflon films coated etched aluminum surfaces. *Mater. Lett.* **2008**, *62*, 1226–1229. [[CrossRef](#)]
47. Xu, P.; Li, X. Fabrication of TiO₂/SiO₂ superhydrophobic coating for efficient oil/water separation. *J. Environ. Chem. Eng.* **2021**, *9*, 105538. [[CrossRef](#)]
48. Barati Darband, G.; Aliofkhaezrai, M.; Khorsand, S.; Sokhanvar, S.; Kaboli, A. Science and engineering of superhydrophobic surfaces: Review of corrosion resistance, chemical and mechanical stability. *Arab. J. Chem.* **2020**, *13*, 1763–1802. [[CrossRef](#)]
49. Parvate, S.; Dixit, P.; Chattopadhyay, S. Superhydrophobic surfaces: Insights from theory and experiment. *J. Phys. Chem. B* **2020**, *124*, 1323–1360. [[CrossRef](#)]
50. Lin, N.; Berton, P.; Moraes, C.; Rogers, R.D.; Tufenkji, N. Nanodarts, nanoblades, and nanospikes: Mechano-bactericidal nanostructures and where to find them. *Adv. Colloid Interface Sci.* **2018**, *252*, 55–68. [[CrossRef](#)]

Disclaimer/Publisher's Note: The statements, opinions and data contained in all publications are solely those of the individual author(s) and contributor(s) and not of MDPI and/or the editor(s). MDPI and/or the editor(s) disclaim responsibility for any injury to people or property resulting from any ideas, methods, instructions or products referred to in the content.